Journal
Geocarto International >
Latest Articles

Articles

Applicability and performance of statistical index, certain factor and frequency ratio models in mapping landslides susceptibility in Rwanda

Lanhai Li, Lamek Nahayo, Gabriel Habiyaremye & Mupenzi Christophe

Received 17 Sep 2019, Accepted 12 Feb 2020, Published online: 21 Feb 2020

Download citation https://doi.org/10.1080/10106049.2020.1730451

Abstract

Formulae display: MathJax

The reduction of landslide losses requires appropriate method to reveal prone areas, causal factors and future occurrence likelihood. This study compared the effectiveness of the Statistical Index (SI), Certain Factor (CF) and Frequency Ratio (FR) models on landslide susceptibility mapping for Rwanda. Historical record and extensive field surveys generated an inventory map of 336 points. Thereafter, 245 and 91 points were randomly selected for building susceptibility and validation, respectively. Ten causal factors: elevation, slope angles, aspects, lithology, soil texture, distance to rivers, distance to roads, rainfall, land use/cover and normalized difference vegetation Index were analyzed. The area under curve (AUC) method revealed the training accuracies of 89.2%, 85.3% and 82.1% for the FR, CF and SI methods, respectively. And the prediction accuracies were 88.7%, 83.9% and 80.2% for the FR, CF and SI methods, respectively. Therefore, the FR performed well in landslide susceptibility mapping over the study area.

Keywords: Bivariate and multivariate statistical models, GIS, landslide susceptibility, Rwanda

1. Introduction

Landslides are among the global geological hazards responsible for considerable human injury and death, natural resources degradation, infrastructure damage, and loss of cultural and natural heritage (Fan et al. 2018; Frodella et al. 2018), which are characterized by sudden destruction and difficult prediction. Landslide occurrence depends on intrinsic and extrinsic variables. The intrinsic variables include soil depth and soil type, slope angles, slope aspect and slope curvature, elevation, land use and drainage patterns, etc., while extrinsic variables include rainfall, earthquake and volcanic activities (Bozzano et al. 2011; Yiping et al. 2014; Jaafari et al. 2015; Tian et al. 2017; Kim et al. 2018). Landslide susceptibility is defined as the spatial probability of landslide occurrence (Van Westen et al. 2008). The application of appropriate method to map landslide susceptibility will help to reveal the prone areas, causal factors and future occurrence likelihood, as well as reducing the losses of human life and properties caused by landslide occurrence.

In the literature, several GIS-based approaches were employed to map landslide susceptibility. These include not limited to the bivariate and multivariate method (Pham et al. 2017), ; Fan et al. 2018; Nsengiyumva et al. 2018); weight of evidence (Xu et al.

2012; Chen et al. 2017; Cui et al. 2017), random forest (Yiping et al. 2014; Hong et al. 2016), fuzzy logic and artificial neural networks (Kim et al. 2010; Pham et al. 2017), ; Ambrosi et al. 2018; Kumar et al. 2018; analytical hierarchy process (Shahabi et al. 2014; Banerjee et al. 2018), evidential belief function (Yalcin 2008; Che et al. 2012; Cui et al. 2017), frequency ratio (Sharma et al. 2014; Pourghasemi and Rossi 2017), certain factor and support vector machine (Domínguez-Cuesta et al. 2010; Urlaub et al. 2013; Li et al. 2014).

In Rwanda, landslide is the frequently recorded hazard, specifically in the northwestern areas due to frequent and torrential rainfall, high altitude and inappropriate land management which facilitate the runoff. This causes severe losses and damages among people, their belongings and natural resources degradation as well (Piller 2016; Nsengiyumva et al. 2018). Studies on mapping landslide susceptibility in Rwanda are still few, and some were mainly statistical or limited to case studies. Previously, the study of Lamek et al. (2019) compared the effectiveness of the Analytic Hierarchy Process and Certain Factor Models in mapping landslide susceptibility and the study was limited to one case: western Rwanda. In addition, the study of Nsengiyumva et al., (2018) employed the Spatial Multi-criteria evaluation models to map landslide susceptibility over the entire Rwandan territory.

Based on the fact that the above bivariate and multivariate statistical models have been in use across several parts of the world and provided successful results, the authors attempted to test their performance in Rwanda. Then among others, this study firstly applied the Statistical Index, Frequency Ratio and Certain Factor models and compared their effectiveness in mapping landslide susceptibility in Rwanda. Moreover, the authors recognized the fact that Rwanda is a small and poor country with a hilly landscape, commonly known as “land of thousand hills” which exposes the country to easy runoff facilitated by its heavy rainfall intensity taking almost a half of the year. Then, as the study was the first attempt, the authors chose to employ three models and several factors in order to select the best model performing in landslide susceptibility mapping and key driving factors. Therefore, this landslide susceptibility mapping would be useful to policy makers to understand landslide hazard mitigation and adaptation needs in Rwanda.

2. Study area

Rwanda is a poor and densely populated East African country with a green and mountainous landscape. The country (Figure 1(a)) is bordered by the Democratic Republic of Congo in the west, Uganda in the north, Burundi in the south and Tanzania in the east. The country’s rainy season starts from March to end of May and late September to early December. The average monthly rainfall is about 110-200 mm. The dry season ranges from late December to end of February and from June to early September. The average monthly temperature is 19-27 °C (Nsengiyumva et al. 2018).

Figure 1. Map indicating the (a) geographical location of Rwanda in Africa and (b) its neighbouring countries.

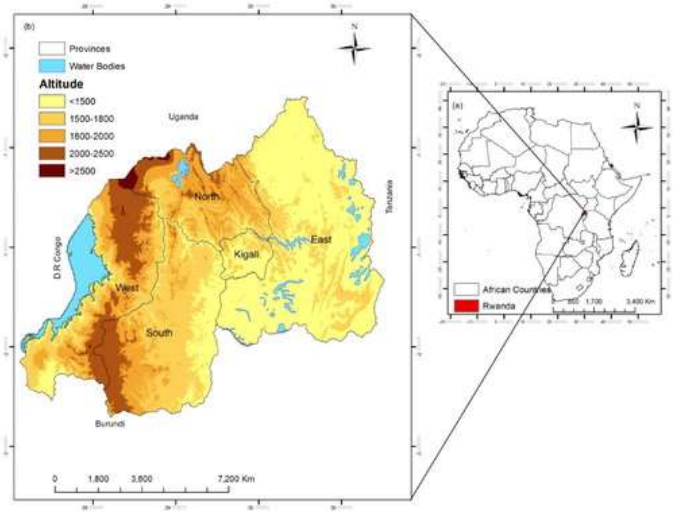

Display full size

In Rwanda, mainly at the north-western parts, the land sharply drops into waters. The land falls across the central plateau in the eastern and its grassy highlands are the core areas of settlements. This topography exposes the residents to runoff since the land is not well covered/protected. This in turn causes the occurrence of landslide and its associated losses (Ntwali et al. 2016). In addition, high rainfall intensity and population pressure on land expose the hilly topography to several runoff risks in Rwanda. This generates severe environmental disasters and encroachment on fragile ecosystems (Piller 2016; Nsengiyumva et al. 2018).

The available data from the Rwanda's former Ministry of Disaster Management and Refugee Affairs (MIDIMAR 2017) indicated that since 1960, landslides were recorded in Rwanda and the number comparatively rose in 2000 onwards. For example, between 2010 and 2017, more than 10,000 people were affected by landslides (killed, injured and homeless), 11,328 ha of cropland, 22,134 houses and other infrastructures have been damaged.

3. Data and methods

3.1. Data

3.1.1. Landslides inventory map

The study of Van Western et al. (2008) suggested that for landslide susceptibility assessment, it is good to consider past distribution of landslide. This is due to the fact that, the factors that led to past landslide occurrence in the area of study if reoccurred, may result from the same factors. For the present study, historical record and field surveys identified 336 past landslides from which the landslide inventory map (Figure 2) was prepared.

Figure 2. Landslides inventory map representing the training data (red color) and validating data (green color).

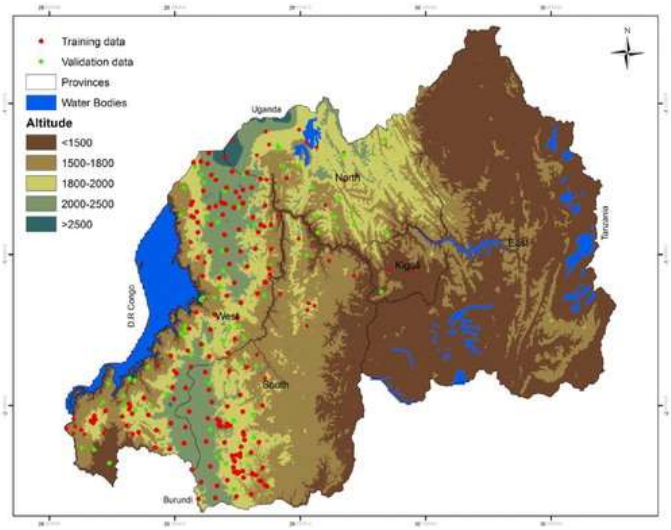

Display full size

As recently reported (Chung and Fabbri 2003), the model's validation cannot be possible unless the datasets are divided into training and testing datasets. Therefore, for this study, the obtained inventory points were randomly divided into 245 locations (73%) for building the model as training datasets, and 91 locations (27%) were applied in the training exercise as the testing datasets. This ratio of 73/27 for dividing the data for generating the training and testing datasets based on the suggestions of recent landslide susceptibility mapping studies (Pourghasemi et al. 2012). Pham et al. 2015.

3.1.2. Landslides conditioning parameters

One of the key points in the assessment of landslide susceptibility is the selection of the conditioning factors. These conditioning factors should be complete, measurable, operational and non-redundant (Domínguez-Cuesta et al. 2010; Hong et

al. 2016; Chen et al. 2017).

For this study, ten causal factors namely: elevation, slope angles, slope aspects, rainfall, lithology, soil texture, distance to rivers, distance to roads, rainfall, land use and land cover (LULC) and normalized difference vegetation Index (NDVI) were employed. These factors were selected with reference to the literature review and field observation. In addition, recent studies on landslide in Rwanda (Nduwayezu et al. 2015; Nsengiyumva et al. 2018) were associated with the national disaster risk management policy, and contingency plan for flood and landslide in Rwanda (MIDIMAR 2014) and the landslide hazard and risk assessment of the United Nations Office for Disaster Reduction (UNISDR 2013) as expert knowledge.

Elevation, slope angles and slope aspects employed by this study (Figure 3(a,b,c)) were derived from Digital Elevation Model (DEM) of 30 m resolution. These datasets were acquired from the United States Geological Survey Earth Explorer (USGS 2018). The obtained five elevation classes were: 915-1,541 m, 1,541-1,833 m, 1,833-2,194 m, 2,194-2,804 m, and 2,204-4,486 m. The slope angles were classified as: 0-5°, 5-15°, 15-30°, and 30-45° and >45°. Whereas nine slope aspects were listed as: flat (−1-39), northeast (39-79°), east (79-119°), southeast (119-159°), south (159-199°), southwest (199-239°), west (239-279°), northwest (279-319°) and north (319-360°).

Figure 3. Landslides triggering factors: (a) elevation, (b) slope angles, (c) slope aspects and (d) monthly rainfall.

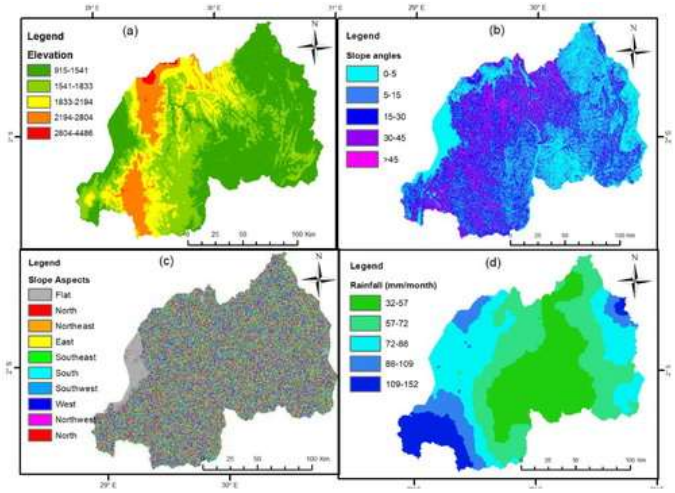

Display full size

In Rwanda, more than 70% of landslide occurrence and losses are rainfall-induced (MIDIMAR 2014). The authors recognized this fact and then added rainfall among the employed datasets to reveal its contribution to landslide susceptibility in this study area. Monthly precipitation data were interpolated by using 28 years (1990–2018) rainfall data collected from meteorological stations operating countrywide. These data were provided by the Rwanda Meteorology Agency (RMA 2018). The mean monthly rainfall (Figure 3(d)) was ranged as: 32-57 mm, 57-72 mm, 72-88 mm, 88-109 mm and 109-152 mm. The study employed monthly rainfall due to the reason that hourly or daily rainfall could not be available since some years had incomplete datasets. Thus, authors preferred to employ monthly data which were complete from 1990 to 2018.

It is reported that each lithology and soil unity influence the type and intensity of landslide, and that their classification helps to demonstrate each class's contribution (Bozzano et al. 2011). The Rwandan lithological and geological features employed by this study (Figure 4(a,b)) were derived from Rwandan geological, mining and soil databases (Rushemuka et al. 2014). The obtained ten lithology classes were: volcanic ash, colluvial, schist, granite, quartzite, fluvial, basic igneous rock, organic, water bodies and basalt. Whereas five soil texture classes were: loamy, sand clay loam, clay loam, sand and clay. For this study, the distance to roads were added among the datasets due to the fact that, cutting of slopes for roads construction or road widening in hilly regions can cause slope failures then lead to landslides losses among the exposed nearby populations (Chen et al. 2017). In addition, people located close to rivers experience severe losses and damages during landslide occurrence (Cui et al. 2017).

Figure 4. Landslide triggering factors: (a) lithology, (b) soil texture, (c) distance to roads and (d) distance to rivers.

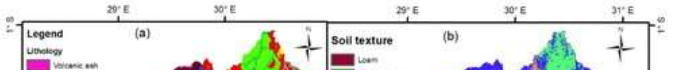

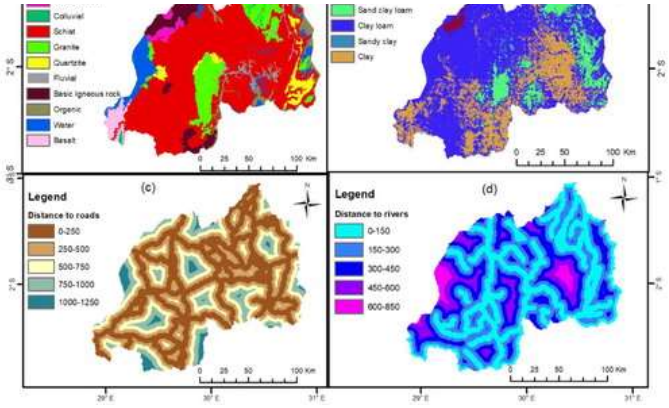

Display full size

The buffers created for distance to roads (Figure 4(c)) in meters were: 0-250 m, 250-500 m, 500-750 m, 750-1,000 m and 1,000-1,250 m. The distance to rivers (Figure 4(d)) in meters was: 0-150 m, 150-300 m, 300-450 m, 450-600 m and 600-850 m. The shapefiles of rivers and roads were acquired from an online database (http://www.diva-gis.org/gdata). Both distance to rivers and distance to roads were produced by creating Euclidean distance in ArcMap-Spatial Analyst extension.

The type of the land coverage represents the likelihood of the land exposure to erosion and other runoff risks including landslide. For this study, land use and land cover (LULC) map of July 2018 was produced from multispectral Landsat-8 Operational Land Imager (OLI) images. These images were acquired from the United States Geological Survey Earth Explorer (USGS 2018). The land cover/use map was classified with supervised maximum classification based on the East African Classification of Regional Center for Mapping and Resources Development (Belle et al. 2014). Then, five LULC classes (Figure 5(a)) were produced and the dominant classes are cropland and forest which occupy 60.4 and 15.4 percent of the total land, respectively. The Normalized Difference Vegetation Index (NDVI) gives a quantitative estimate on the relationship between landslides and the vegetation density (Shi-Biao et al. 2009). The NDVI (Figure 5(b)) used by the present study was acquired from the Moderate Resolution Imaging Spectroradiometer (MODIS, 250 M resolution) downloaded from an online database (ladsweb.nasacom.nasa.gov/data/html). The calculation of NDVI values based on the following equation:

$$\mathrm{NDVI} = \frac{IR - R}{IR + R} \quad (1)$$

Figure 5. Landslide triggering factors: (a) land use and land cover and (b) normalized difference vegetation index.

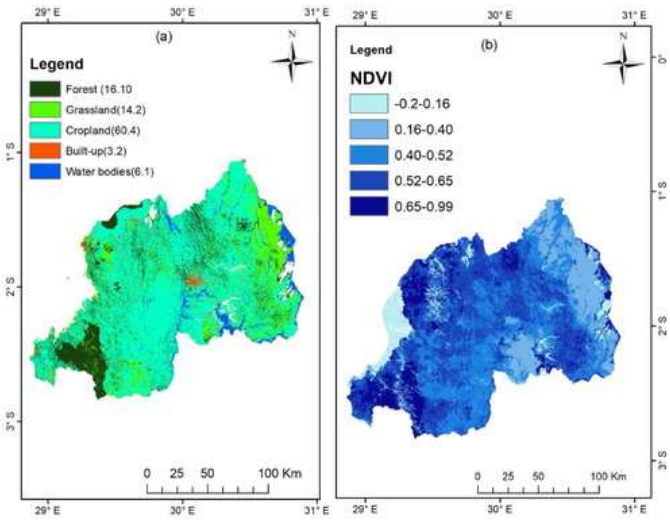

Display full size

Where IR is the infrared portion of electromagnetic spectrum and R value is the red portion of electromagnetic spectrum. This sentence should be placed below equation 1 not below Figure 5.

3.2. Methods

As described in section 3.1.2, the authors employed ten factors which are likely associated to landslide occurrence in Rwanda. Their choice based on the literature review, field observation and experts' opinion on the landslide occurrence and its triggering factors. As shown in the Figure 6 below, the study used three modelling approaches namely the Statistical Index, Certain factor and Frequency Ratio models. These approached helped to demonstrate the relationship between landslide occurrence and the selected triggering factors. The methods also enabled the authors to spatially distribute landslide susceptibility in Rwanda. The authors also calculated the correlation between the employed causal factors in order to indicate the extent to which each factor correlates with the other to cause landslide occurrence in the study area.

Figure 6. Flowchart indicating the methodology applied to this study.

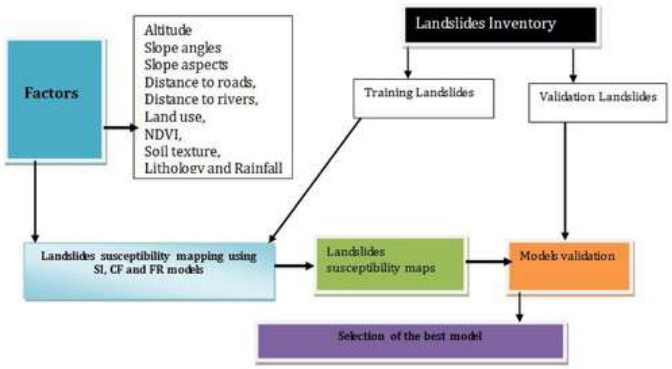

Display full size

3.2.1. Statistical index model

The Statistical Index (SI) is accepted as bivariate statistical method (Van Westen et al. 1997). The model has a basis requiring calibration from correlation between known incidents. In the model, the weighting value for each conditioning factor class is defined as the natural logarithm of the landslides density in a class divided by landslides density in the entire map (Van Westen et al. 1997). The statistical index is calculated as follows:

$$Wij = In\left(\frac{DensClasij}{DensMap}\right) = In\left[\frac{\frac{N\,pix\,(Sij)}{N\,pix\,(Nij)}}{\frac{\sum_j N\,pix\,(Sij)}{\sum_j Npix\left(Nij\right)}}\right] \quad (2)$$

Where W_{ij} is the weight for class j within the triggering factor map *I*, DensClasij is density of landslides in class *j* within the triggering factor map *I*, *DensMap* is the density of landslides in the entire map, N_{pix} (S_{ij}) is the number of pixels in class *j* within the triggering factor map *I* and N_{pix} (N_{ij}) is the number of pixels in class *j* within the triggering factor map *i*. Hence, for this study, based on the above formula, landslide susceptibility map was produced by using the following equation.

$$LSIsi = Wsi\ (elevation) + Wsi\ (slope\ angle) + Wsi\ (slope\ aspects) + Wsi\ (rainfall) + Wsi\ (lithology) + Wsi\ (soil\ texture) + Wsi\ (distance\,to\,roads) + Wsi\ (distance\,to\,rivers) + Wsi\ (Land\ Use) + Wsi\ (NDVI) \quad (3)$$

Where LSI_{si} is landslides susceptibility index by statistical index and W_{si} is the weight of each landslides conditioning factor determined by the statistical index model.

3.2.2. Frequency ratio model

The Frequency Ratio (FR) model is used by basing on the assumption that future landslides will reoccur under similar conditions to the past ones. This is the reason why the model suggests that to estimate future occurrence and susceptibility extent, there is a need of considering the relationship between distribution of recent landslides and each of the selected conditioning factors (Kannan et al. 2013; Sharma et al. 2014). For this study, in order to evaluate the contribution of each factor toward landslides occurrence, landslide group was overlaid with thematic data layers separately for calculation of frequency ratio. Then, the values of each factor's frequency ratio were summed to produce landslides susceptibility as follows:

$$LSI = \frac{N\,(si)/\,Npis\,(Ni)}{\sum N\,pix\,(si)/\sum Npis(Ni)}$$

(4)

Where LSI is landslides susceptibility index, N (Si) is the number of landslides in a certain parameter class, N pix (Ni) is the number of pixel in a certain parameter class, Σ N (Si) is the total number of landslides in a certain parameter class and Σ N pix (Ni) is the total number of pixels in a certain parameter class.

The class boundaries for each factor were determined prior to the calculation. Then landslide susceptibility index (LSI) was calculated by adding the frequency ratio of each factor for the given pixel. To ensure compatibility between models with different numbers of factors, the sum was divided by the total number of triggering factors employed as follows:

$$\mathrm{LSI} = \frac{1}{n}\sum_{i=1}^{n} FRi$$

$$+\frac{\begin{array}{c} FR\,(elevation) + FR\,(slope\ \ angle) + FR\,(slope\ \ aspects) + FR\,(rainfall) + FR\,(lithology) \\ +FR\,(soil\ \ texture) + FR\,(distance\,to\,roads) + FR\,(distance\,to\,rivers) + RF\,(LULC) \\ +\,FR\,(NDVI) \end{array}}{10}$$

(5)

3.2.3. Certain factor model

The Certain Factor (CF) is a rule–based expert system method developed by Shortliffe and Buchanan (1975) for the management of uncertainty in computational studies. The CF model provides probable favorability functions (FF) for integrating heterogeneous data (Shortliffe and Buchanan 1975; Dou et al. 2015) and can be calculated by using the following formula.

$$\mathrm{CF} = \begin{cases} \frac{PPa - PPs}{PPa\,(1-PPs)}, if PPa \geq PPs \\ \frac{PPa - PPs}{PPs(1-PPa)}, if PPa < PPs \end{cases}$$

(6)

Where Ppa is the conditional probability of landslides in class a and PPs is the prior probability of total number of landslides in the study area. The CF values range between −1 and 1, a positive value measures decreasing uncertainty whereas negative values imply an increasing uncertainty of landslides occurrence. In case the CF values equal to 0, no information on the certainty is indicated (Shortliffe and Buchanan 1975). For this study, after obtaining the CF values for classes of the causative factors, these factors were then incorporated into pairwise combination by using the combination rule as follows:

$$\begin{cases} CF1 + CF2 - CF1CF2CF1, CF2 \geq 0 \\ CF1 + CF2 + CF1CF2CF1, CF2 < 0 \end{cases}$$

$$Z = \begin{cases} \\ \frac{CFQ\,1 - CF2}{1 - min\,(CF1, CF2)} CF1, CF2\ opposite\ \ signs \end{cases}$$

(7)

The pairwise combination was carried out until all the CF layers were brought together. The triggering factors were optimized by computing the Z values. If the Z values are positive, they are regarded as possessing high relationship with landslides occurrence. Based on the range of CF values, feature weights were obtained. The weights are estimated as the sum of the ration computed relative causative factors that provide a measurement of certainty in forecasting landslides occurrence (Shortliffe and Buchanan 1975).

4. Results

4.1. Multicollinearity and correlation analysis between landslide causal factors

The authors chose to indicate how the selected causal factors correlate one another and then run a Multicollinearity Analysis which was conducted by the Variance Inflation Factors (VIF) and Tolerance method for the selection of suitable landslide conditioning parameters in the study area. The authors recognized the suggested values of the VIF (>10) and that of tolerance (< 0.1) which show a problem of multicollinearity in conditioning factors (Pourghasemi et al. 2012; Nohani et al. 2019). As indicated in Table 1, the multicollinearity diagnosis indicated no collinearity between the employed ten landslide causal factors.

Table 1. Multicollinearity analysis.

CSV Display Table

In addition, the authors analyzed the correlation between the landslide causal factors with use of Correlation Analysis. This analysis states that positive values (>1) indicate positive correlation with landslide and negative values (<1) reveal negative correlation with landslide (Neuhäuser and Terhorst 2007; Dou et al. 2015).

The results in Table 2 indicated that the highest correlation exists between slope angles and land use and land cover, and between elevation and slope angles at 0.78, respectively. The other high correlation was marked between rainfall and lithology (0.81). The third high correlation was noted between elevation and land use and land cover, and between elevation and rainfall at 0.74, respectively. This expresses that within zones of the study area where these causal factors (elevation, slope angles, rainfall and land use and land cover) are dominating; there is high likelihood of exposure to landslide.

Table 2. Causal factors' correlation analysis.

CSV Display Table

4.2. Landslide susceptibility mapping by statistical index (SI) model

The results on the spatial relationship between each landslide conditioning factor and landslide occurrence by the SI Model are shown in Table 3. The results indicated that high SI values of elevation are mainly in the classes of 2,194-2,804 m (0.82) and 1,833-2,194 m (0.42). For the slope angles, highest SI value (0.36) was noticed for the slope ranging between 30 and 45 degrees. For the slope aspects, the southwest (0.23), west (0.64), northwest (0.49) and north (0.21) had highest SI values (Table 3). With

regard to rainfall, the ranges of 72-88 mm, 88-109 mm and 109-152 mm indicated higher SI scores of 0.84, 0.67 and 0.78, respectively. Also, the results in Table 3 pointed out the schist as the dominating lithological class with high SI value (0.71).

Table 3. Spatial relationship between landslide triggering factors and its susceptibility by SI, CF and FR models.

CSV Display Table

In addition, among other soil textures, the SI model indicated the clay loam (0.12 in Table 3) as the major soil texture class which conditions landslide occurrence in Rwanda. For the land use and land cover, the results in Table 3 revealed high SI values of 2.82, 1.63 and 1.38 for grassland; cropland and forest, respectively. The obtained relationship between NDVI and landslides occurrence in Rwanda (Table 3) revealed higher likelihood of landslide occurrence within NDVI scope of 0.53-0.65 due to its high SI value (0.89). Finally, the SI model (Table 3) revealed that the closer to roads and rivers, the higher susceptibility to landslides. This is due to higher SI ranks of the distance to rivers' classes of 0-150 m (0.59) and 150-300 m (0.04) and roads' classes of 0-250 m (1.21) and 250-500 m (0.01). Kindly, place Figure 7 here since it i srelated to LSM by SI model.

4.3. Landslide susceptibility mapping by frequency ratio (FR) model

The results in Table 3 by the Frequency Ratio model revealed high values of 1.97 and 1.74 for the elevation classes: 2,194-2,804 m and 1,833-2,194 m, respectively. For the slope angles and slope aspects, the results in Table 2 indicated that slope angles: 30-45° and >45° have highest FR values of 1.29 and 2.58, respectively. While the slope aspects namely: west (6.38), northwest (2.92) and north (4.67), respectively, had higher FR values. In term of rainfall, Table 1 showed higher FR values by the rainfall ranges of 72-88 mm (2.31), 88-109 mm (1.55) and 109-152 mm (1.39). Similarly to the Statistical Index Model (Table 3), the results by the Frequency Ratio (Table 3) confirmed the schist (FR value: 4.72) as the major lithological class which triggers the occurrence of landslide in Rwanda than other lithological classes (Table 3). Regarding the soil texture and its relationship with landslide occurrence in Rwanda, the Frequency Ratio model (Table 3) highlighted clay loam (2.69), loam (1.77) and clay (1.23) as the soil texture classes with advanced contribution to landslide occurrence. In addition, the results in Table 3 revealed high FR value from the NDVI class of 0.16-0.40 (2.89). For the land use, Table 3 showed that the cropland (1.69), grassland (2.82) and forest (1.38) had advanced FR values. Moreover, the results in Table 3 indicated higher FR values of 0.95 and 0.86 for the distance to rivers ranging between of 450 and 600 m, and from 300 to 450 m, respectively. Finally, for the distance to roads, high FR values of 2.57 and 1.84 were observed for the ranges of 0-250 m and 250-500 m, respectively.

Kindly, place Figure 8 here, it show the map of Landlside susceptibility by FR model.

4.4. Landslide susceptibility mapping by certain factor (CF) model

The spatial relationship between landslide occurrence and the selected causal factors estimated by CF model (Table 3) revealed that elevation classes: of 2,194-2,804 m and 1,833-2,194 m registered higher CF records of 0.72 and 0.59, respectively. The results in Table 3 showed that the slope angles ranging between 30 and 45 degrees had the highest CF value of 0.77. For the slope aspects, the CF model (Table 3) highlighted the west (0.89), northwest (0.63), north (0.44) and south (0.43) as the slope aspects with high CF values compared to other slope aspects. For the relationship between landslide occurrence and rainfall in Rwanda, the results by the Certain Factor model (Table 3) showed high values of 0.71, 0.38 and 0.27 for rainfall ranges of 72-88 mm, 88-109 mm and 109-152, respectively. In addition, the results in Table 3 identified the schist (0.82) and clay loam (0.24) as the lithology and soil texture classes with highest CF values compared to other classes. With regard to the land use and land cover, the CF model (Table 3) revealed high values of grassland (0.63), cropland (0.51) and forest (0.18). While the NDVI class of 0.53-0.65 revealed the highest CF value of 0.68 compared to other NDVI classes. Moreover, for the distance to rivers, highest CF values were found in the ranges of 0-150 m (CF: 0.88) and 150-300 m (CF: 0.72). Finally, the distance to roads ranging between 0-250 m and 250-500 m generated high CF values of 0.96 and 0.72, respectively (Table 3). Please, locate Figure 9 here, it corresponds to LSM by CF model.

4.5. Validation of landslide susceptibility maps

The validation of the predictive models is an essential requirement to check the accuracy of the produced landslide susceptibility maps (Shahabi et al. 2014). The authors considered the fact that several methods are under use for assessing the

performance of landslide susceptibility mapping models. Among others, the Area under the Receiver Operating Characteristic Curve (AUROC) was mentioned to efficiently visualize and compare models' performance (Frattini et al. 2010). Therefore, the authors selected this method and then assessed its success in this area due to its recent success across different areas. This can be confirmed by recent studies (Kim et al. 2010; Sharma et al. 2014; Banerjee et al. 2018) which indicated that the validity of landslides susceptibility map was graphically ascertained with the use of the area under curve (AUC) method, and that the method proved its usefulness in validating the prediction performance of the model.

In this study, 73% of 245 landslides were randomly selected as training datasets for susceptibility building, and the remaining (27% of 91 landslides) also randomly selected, were used as validation datasets. The results in Figure 10 indicated the results on the success rate and prediction capability of landslide susceptibility maps prepared by SI, CF and FR models. The success rate was obtained by comparing the training data with the landslide susceptibility maps. Whereas each model's prediction rate was validated by comparing landslide susceptibility maps with the validation data. The results (Figure 10(a)) showed that the FR model has the highest training accuracy (89.2%), followed by CF model (85.3%) then the SI model with the lowest training accuracy of 82.1 percent. In addition, the prediction rate in Figure 10(b) revealed that the FR model had the highest prediction accuracy (86.7%) compared to the CF (83.9%) and SI (80.2%) models. Therefore, the FR is the best performer for landslide susceptibility mapping in this area. It would be good if Figure 10 is placed here to reveal the validation Figure.

5. Discussion

This study analyzed landslide susceptibility by using the bivariate and Multivariate Statistical models (Statistical Index, Certain Factor and Frequency Ratio) and compared their prediction capabilities for Rwanda. The three methods helped to spatially categorize the study area into varied degrees of landslide susceptibility (Figures 5–7). These models based on integration of ten identical and individual weighted triggering factors and landslide inventory (see sections 3.1.2). Each of the employed models (SI, CF and FR) has its own advantages in producing landslide susceptibility. The statistical index model combines the causal factor maps of weighted class with landslide distribution. Its advantage is the quantitative and objective manner of susceptibility measurement which helps to indicate the major factors that strongly influence landslide occurrence (Cui et al. 2017). The frequency ratio model employs both subclass and causal factor weights with the aim of promoting factors with a great importance to landslide occurrence (Shahabi et al. 2014). Whereas the certain factor model has the capability function of dealing with the combination of different data layers, heterogeneity and uncertainty of the input data (Fan et al. 2017).

Figure 7. Landslides susceptibility map produced by the Statistical Index Model.

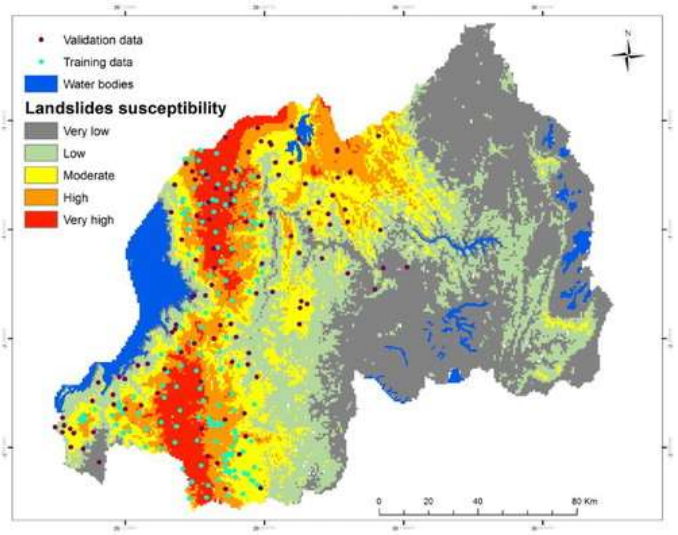

Display full size

Previous studies (Hong et al. 2016; Cui et al. 2017; Fan et al. 2017) which employed these methods have proved their ability of mapping landslide susceptibility. These studies assessed the performance of the Certain Factor, Frequency Ratio and Statistical

Index models by using AUROC method. And the method proved its success and indicated the CF and FR as the best performers compared to SI model. Similarly, for this study, the accuracy and prediction of mapping of landslide susceptibility generated by the Certain Factor, Frequency Ratio and Statistical Index models highlighted the FR with high performance followed by the CF then the SI model. This is justified by the validation results (Figure 10(a, b)) which showed that the FR model has the highest prediction and training accuracies of 89.2% and 86.7%, respectively. The SI and FR also generated good prediction and training accuracies higher than 75 percent. This expresses that all three methods can be applied in Rwanda in mapping landslide susceptibility with high preference attributed to the Frequency Ratio model.

The results on landslide susceptibility produced by the three employed methods (Figures 7–9) and the causal factors correlation analysis (Table 2) confirmed that the areas of Rwanda with high elevation, slope, rainfall and lithology along with poor land management are likely susceptible to landslide. In addition, areas close to roads mainly in north-western Rwanda (Figure 5(c)) are highly prone to landslide (Figures 7–9). For the land use and land cover, it is shown that areas with high percentage of cropland are susceptible to landslide. This high susceptibility can be the result of the existing policy on producing rotational crops other than permanent crops and expanding urbanization/settlement which expose the available land to erosion and landslide. Thus, it is good to expand forestland and/or permanent cropland in order to protect the land from erosion and other runoff associated consequences including landslide.

Figure 8. Landslides susceptibility map prepared by the Frequency Ratio model.

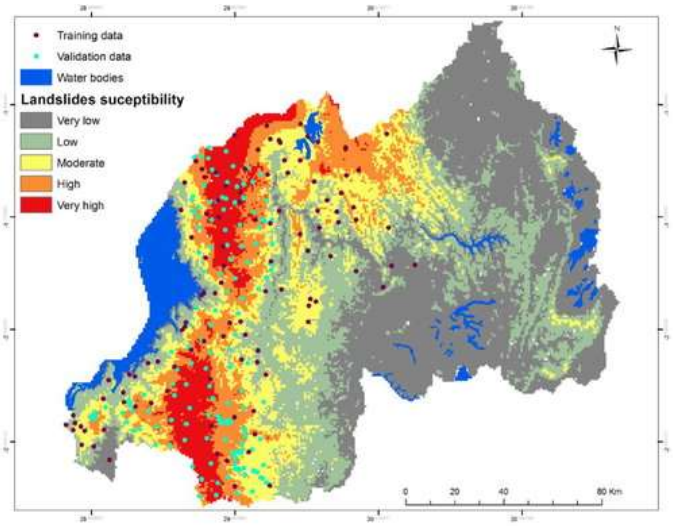

Display full size

Figure 9. Landslides susceptibility map prepared by using Certain Factor model.

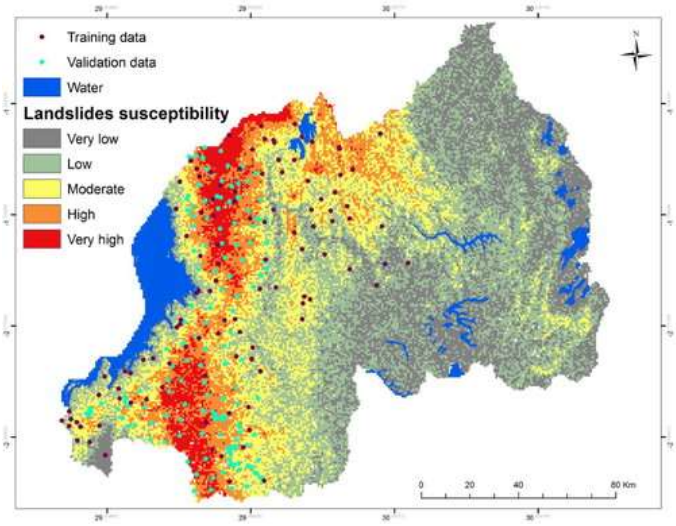

Display full size

Figure 10. Success rate (a) and (b) prediction rate of the SI, CF and FR models.

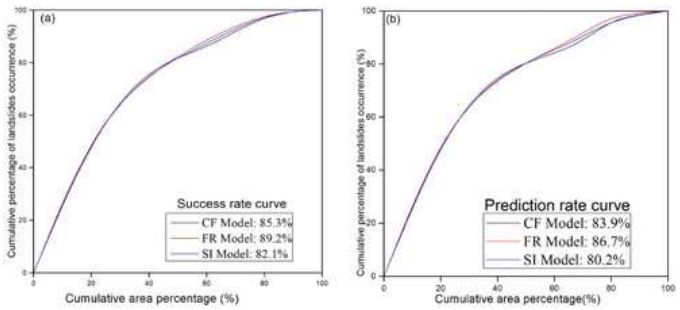

Display full size

The results of this study agree with the report of Lamek et al. (2019) and Nsengiyumva et al. (2018) which indicated that Rwandan high elevation, slope and rainfall along with inappropriate use and management of the land are the primary factors leading to the occurrence of landslide. Therefore, in order to minimize the occurrence and losses of landslide in Rwanda, it is good to ensure the practice of agroforestry and bench terraces. Also, the rain harvest and approaching the local community to improve its awareness on disaster causes, impact and ways of adaptation would reduce the losses.

6. Conclusion

This study compared the performance of three bivariate and multivariate statistical approaches (Statistical Index, Certain Factor and Frequency Ratio) in mapping landslide susceptibility in Rwanda. These models are employed for the first time in this area and their results are quite promising in landslide susceptibility mapping and predicting. Regardless the fact that all three methods produced good results in mapping landslide susceptibility, the findings highlighted the Frequency Ratio as the best approach compared to the Certain Factor and Statistical Index approaches. All methods indicated that elevation, rainfall, slope and poor land management are the major factors which condition the occurrence of landslide in Rwanda. It is concluded that landslide susceptibility maps produced by using all three models represent good prediction capacity. This can be a good indicator which suggests their application to other landslide prone regions with similar settings. This study will enable policy makers to better understand landslides hazard mitigation and adaptation needs based on the susceptibility magnitude and triggering factors.

Acknowledgment

The authors are grateful for the support in data collection and analysis from the Chinese Academy of Sciences (CAS) Research Centre for Ecology and Environment of Central Asia.

Disclosure statement

No potential conflict of interest was reported by the author(s).

Data availability

All data used by this study are available upon request from the corresponding author.

References

1. Ambrosi C, Strozzi T, Scapozza C, Wegmüller U. 2018. Landslide hazard assessment in the Himalayas (Nepal and Bhutan) based on Earth-Observation data. Eng Geol. 237:217–228. [Crossref], [Web of Science ®], [Google Scholar]

2. Banerjee P, Ghose MK, Pradhan R. 2018. Analytic hierarchy process and information value method-based landslide susceptibility mapping and vehicle vulnerability assessment along a highway in Sikkim Himalaya. Arab J Geosci. 11(7):139. [Crossref], [Web of Science ®], [Google Scholar]

3. Belle P, Aunay B, Bernardie S, Grandjean G, Ladouche B, Mazué R, Join J.-L. 2014. The application of an innovative inverse model for understanding and predicting landslide movements (Salazie cirque landslides, Reunion Island). Landslides. 11(3):343–355. [Crossref], [Web of Science ®], [Google Scholar]

4. Bozzano F, Lenti L, Martino S, Paciello A, Mugnozza GS. 2011. Evidences of landslide earthquake triggering due to self-excitation process. Int J Earth Sci (Geol Rundsch). 100(4):861–879. [Crossref], [Web of Science ®], [Google Scholar]

5. Che VB, Fontijn K, Ernst GG, Kervyn M, Elburg M, Van Ranst E, Suh CE. 2012. Evaluating the degree of weathering in landslide-prone soils in the humid tropics: the case of Limbe, SW Cameroon. Geoderma. 170:378–389. [Crossref], [Web of Science ®], [Google Scholar]

6. Chen W, Pourghasemi HR, Kornejady A, Zhang N. 2017. Landslide spatial modeling: introducing new ensembles of ANN, MaxEnt, and SVM machine learning techniques. Geoderma. 305:314–327. [Crossref], [Web of Science ®], [Google Scholar]

7. Chung C.-JF, Fabbri AG. 2003. Validation of spatial prediction models for landslide hazard mapping. Nat Hazards. 30(3):451–472. [Crossref], [Web of Science ®], [Google Scholar]

8. Cui K, Lu D, Li W. 2017. Comparison of landslide susceptibility mapping based on statistical index, certainty factors, weights of evidence and evidential belief function models. Geocarto Int. 32(9):935–955. [Taylor & Francis Online], [Web of Science ®], [Google Scholar]

9. Domínguez-Cuesta MJ, Jiménez-Sánchez M, Colubi A, González-Rodríguez G. 2010. Modelling shallow landslide susceptibility: a new approach in logistic regression by using favourability assessment. Int J Earth Sci (Geol Rundsch). 99(3):661–674. [Crossref], [Web of Science ®], [Google Scholar]

10. Dou J, Bui DT, Yunus AP, Jia K, Song X, Revhaug I, Xia H, Zhu Z. 2015. Optimization of causative factors for landslide susceptibility evaluation using remote sensing and GIS data in parts of Niigata, Japan. PLoS One. 10(7):e0133262. [Crossref], [PubMed], [Web of Science ®], [Google Scholar]

11. Fan W, Wei X.-s, Cao Y.-b, Zheng B. 2017. Landslide susceptibility assessment using the certainty factor and analytic hierarchy process. J Mt Sci. 14(5):906–925. [Crossref], [Web of Science ®], [Google Scholar]

12. Fan X, Zhan W, Dong X, van Westen C, Xu Q, Dai L, Yang Q, Huang R, Havenith H.-B. 2018. Analyzing successive landslide dam formation by different triggering mechanisms: The case of the Tangjiawan landslide, Sichuan, China. Eng Geol. 243:128–144. [Crossref], [Web of Science ®], [Google Scholar]

13. Frattini P, Crosta G, Carrara A. 2010. Techniques for evaluating the performance of landslide susceptibility models. Eng Geol. 111(1–4):62–72. [Crossref], [Web of Science ®], [Google Scholar]

14. Frodella W, Ciampalini A, Bardi F, Salvatici T, Traglia FD, Basile G, Casagli N. 2018. A method for assessing and managing landslide residual hazard in urban areas. Landslides. 15(2):183–197. [Crossref], [Web of Science ®], [Google Scholar]

15. Hong H, Pourghasemi HR, Pourtaghi ZS. 2016. Landslide susceptibility assessment in Lianhua County (China): a comparison between a random forest data mining technique and bivariate and multivariate statistical models. Geomorphology. 259:105–118. [Crossref], [Web of Science ®], [Google Scholar]

16. Jaafari A, Najafi A, Rezaeian J, Sattarian A, Ghajar I. 2015. Planning road networks in landslide-prone areas: a case study from the northern forests of Iran. Land Use Policy. 47:198–208. [Crossref], [Web of Science ®], [Google Scholar]

17. Kannan M, Saranathan E, Anabalagan R. 2013. Landslide vulnerability mapping using frequency ratio model: a geospatial approach in Bodi-Bodimettu Ghat section, Theni district, Tamil Nadu, India. Arab J Geosci. 6(8):2901–2913. [Crossref], [Web of Science ®], [Google Scholar]

18. Kim D, Im S, Lee SH, Hong Y, Cha K.-S. 2010. Predicting the rainfall-triggered landslides in a forested mountain region using TRIGRS model. J Mt Sci. 7(1):83–91. [Crossref], [Web of Science ®], [Google Scholar]

19. Kim HG, Lee DK, Park C, Ahn Y, Kil S.-H, Sung S, Biging GS. 2018. Estimating landslide susceptibility areas considering the uncertainty inherent in modeling methods. Stoch Environ Res Risk Assess. 32(11):2987–3019. [Crossref], [Web of Science ®], [Google Scholar]

20. Kumar V, Gupta V, Jamir I, Chattoraj SL. 2018. Evaluation of potential landslide damming: Case study of Urni landslide, Kinnaur, Satluj valley, India. Geosci Front. 10(2):753–767. [Crossref], [Web of Science ®], [Google Scholar]

21. Lamek N, Kalisa E, Maniragaba A, Nshimiyimana FX. 2019. Comparison of analytical hierarchy process and certain factor models in landslide susceptibility mapping in Rwanda. Modeling Earth Systems and Environment. 5(3):885–895. [Crossref], [Web of Science ®], [Google Scholar]

22. Li C, Tang H, Ge Y, Hu X, Wang L. 2014. Application of back-propagation neural network on bank destruction forecasting for accumulative landslides in the three Gorges Reservoir Region, China. Stoch Environ Res Risk Assess. 28(6):1465–1477. [Crossref], [Web of Science ®], [Google Scholar]

23. MIDIMAR. 2014. National Contingency for Flood and Landslides, Ministry of Disaster Management and Refugees, (MIDIMAR), Kigali- Rwanda. 47. [Google Scholar]

24. MIDIMAR. 2017. Ministry of Disaster Management and Refugee Affairs. Report on monthly and annual data on disasters countrywide. Kigali, Rwanda. [Google Scholar]

25. Nduwayezu E, Jaboyedoff M, Bugnon P.-C, Nsengiyumva J.-B, Horton P, Derron M.-H. 2015. Meteorological Hazard Assessment and Risk Mitigation in Rwanda. Paper read at EGU General Assembly Conference Abstracts. [Google Scholar]

26. Neuhäuser B, Terhorst B. 2007. Landslide susceptibility assessment using “weights-of-evidence” applied to a study area at the Jurassic escarpment (SW-Germany). Geomorphology. 86(1-2):12–24. [Crossref], [Web of Science ®], [Google Scholar]

27. Nohani E, Moharrami M, Sharafi S, Khosravi K, Pradhan B, Pham BT, Lee S, Melesse AM. 2019. Landslide susceptibility mapping using different GIS-based bivariate models. Water. 11(7):1402. [Crossref], [Web of Science ®], [Google Scholar]

28. Nsengiyumva JB, Luo G, Nahayo L, Huang X, Cai P. 2018. Landslide susceptibility assessment using spatial multi-criteria evaluation model in Rwanda. Int J Environ Res Public Health. 15(2):243. [Crossref], [Web of Science ®], [Google Scholar]

29. Ntwali D, Ogwang BA, Ongoma V. 2016. The impacts of topography on spatial and temporal rainfall distribution over Rwanda based on WRF model. Atmos Clim Sci. 06(02):145–157. [Crossref], [Google Scholar]

30. Pham BT, Bui DT, Indra P, Dholakia M. 2015. Landslide susceptibility assessment at a part of Uttarakhand Himalaya, India using GIS–based statistical approach of frequency ratio method. Int J Eng Res Technol. 4(11):338–344. [Google Scholar]

31. Pham BT, Bui DT, Pourghasemi HR, Indra P, Dholakia M. 2017. Landslide susceptibility assesssment in the Uttarakhand area (India) using GIS: a comparison study of prediction capability of naïve bayes, multilayer perceptron neural networks, and functional trees methods. Theor Appl Climatol. 128(1–2):255–273. [Crossref], [Web of Science ®], [Google Scholar]

32. Pham BT, Bui DT, Prakash I, Dholakia M. 2017. Hybrid integration of Multilayer Perceptron Neural Networks and machine learning ensembles for landslide susceptibility assessment at Himalayan area (India) using GIS. Catena. 149:52–63. [Crossref], [Web of Science ®], [Google Scholar]

33. Piller AN. 2016. Precipitation Intensity Required for Landslide Initiation in Rwanda. United States. https://pdxscholar.library.pdx.edu/honorstheses/27410.15honors. 2901825 S/honors. 2901825 SW Broadway, Portland, OR 97201. [Google Scholar]

34. Pourghasemi HR, Mohammady M, Pradhan B. 2012. Landslide susceptibility mapping using index of entropy and conditional probability models in GIS: Safarood Basin, Iran. Catena. 97:71–84. [Crossref], [Web of Science ®], [Google Scholar]

35. Pourghasemi HR, Pradhan B, Gokceoglu C. 2012. Application of fuzzy logic and analytical hierarchy process (AHP) to landslide susceptibility mapping at Haraz watershed, Iran. Nat Hazards. 63(2):965–996. [Crossref], [Web of Science ®], [Google Scholar]

36. Pourghasemi HR, Rossi M. 2017. Landslide susceptibility modeling in a landslide prone area in Mazandarn Province, north of Iran: a comparison between GLM, GAM, MARS, and M-AHP methods. Theor Appl Climatol. 130(1–2):609–633. [Crossref], [Web of Science ®], [Google Scholar]

37. RMA. 2018. Rwanda Meteorological Agency, Meteo Rwanda Map Room, Climate Data Library. [accessed 2018 Apr 5]. http://www.meteorwanda.gov.rw/maproom. [Google Scholar]

38. Rushemuka PN, Bock L, Mowo JG. 2014. Soil science and agricultural development in Rwanda: state of the art. A review. BASE. 18:142–154. [Google Scholar]

39. Shahabi H, Khezri S, Ahmad BB, Hashim M. 2014. Landslide susceptibility mapping at central Zab basin, Iran: a comparison between analytical hierarchy process, frequency ratio and logistic regression models. Catena. 115:55–70. [Crossref], [Web of Science ®], [Google Scholar]

40. Sharma L, Patel N, Ghose M, Debnath P. 2014. Application of frequency ratio and likelihood ratio model for geo-spatial modelling of landslide hazard vulnerability assessment and zonation: a case study from the Sikkim Himalayas in India. Geocarto Int. 29(2):128–146. [Taylor & Francis Online], [Web of Science ®], [Google Scholar]

41. Shi-Biao B, Jian W, Guo-Nian L, Ping-Gen Z, Sheng-Shan H, Su-Ning X. 2009. GIS-based and data-driven bivariate landslide-susceptibility mapping in the Three Gorges area. China. Pedosphere. 19(1):14–20. [Crossref], [Web of Science ®], [Google Scholar]

42. Shortliffe EH, Buchanan BG. 1975. A model of inexact reasoning in medicine. Math Biosci. 23(3–4):351–379. [Crossref], [Google Scholar]

43. Tian Y, Xu C, Chen J, Hong H. 2017. Spatial distribution and susceptibility analyses of pre-earthquake and coseismic landslides related to the Ms 6.5 earthquake of 2014 in Ludian, Yunan, China. Geocarto Int. 32(9):978–989.

[Taylor & Francis Online], [Web of Science ®], [Google Scholar]

44. UNISDR. 2013. United Nations International Office for Disaster Reduction (UNISDR). Landslide Hazard and Risk Assessment in El Salvador. From shared risk to shared value: the business case for disaster risk reduction. Global Assessment Report on Disaster Risk Reduction. Geneva (CH). p. 288. [Google Scholar]

45. Urlaub M, Talling PJ, Masson DG. 2013. Timing and frequency of large submarine landslides: implications for understanding triggers and future geohazard. Quat Sci Rev. 72:63–82. [Crossref], [Web of Science ®], [Google Scholar]

46. USGS. 2018. United States Geological Survey, Science for a Changing World. [accessed 2017 July]. https://earthexplorer.usgs.gov/. [Google Scholar]

47. Van Westen CJ, Castellanos E, Kuriakose SL. 2008. Spatial data for landslide susceptibility, hazard, and vulnerability assessment: an overview. Eng Geol. 102(3–4):112–131. [Crossref], [Web of Science ®], [Google Scholar]

48. Van Westen CJ, Rengers N, Terlien M, Soeters R. 1997. Prediction of the occurrence of slope instability phenomenal through GIS-based hazard zonation. Geol Rundsch. 86(2):404–414. [Crossref], [Google Scholar]

49. Xu C, Xu X, Dai F, Xiao J, Tan X, Yuan R. 2012. Landslide hazard mapping using GIS and weight of evidence model in Qingshui river watershed of 2008 Wenchuan earthquake struck region. J Earth Sci. 23(1):97–120. [Crossref], [Web of Science ®], [Google Scholar]

50. Yalcin A. 2008. GIS-based landslide susceptibility mapping using analytical hierarchy process and bivariate statistics in Ardesen (Turkey): comparisons of results and confirmations. Catena. 72(1):1–12. [Crossref], [Web of Science ®], [Google Scholar]

51. Yiping W, Cong C, Gaofeng H, Qiuxia Z. 2014. Landslide stability analysis based on random-fuzzy reliability: taking Liangshuijing landslide as a case. Stoch Environ Res Risk Assess. 28(7):1723–1732. [Crossref], [Web of Science ®], [Google Scholar]